This article was downloaded by: [Isfahan University of Technology]
On: 25 June 2015, At: 07:20
Publisher: Taylor & Francis
Informa Ltd Registered in England and Wales Registered Number: 1072954 Registered office: Mortimer House, 37-41 Mortimer Street, London W1T 3JH, UK

Materials Research Letters
Publication details, including instructions for authors and subscription information:
http://www.tandfonline.com/loi/tmrl20

High-Entropy Alloys: A Critical Review

Ming-Hung Tsai[a] & Jien-Wei Yeh[b]

[a] Department of Materials Science and Engineering, National Chung Hsing University, Taichung 40227, Taiwan

[b] Department of Materials Science and Engineering, National Tsing Hua University, Hsinchu 30013, Taiwan

Published online: 30 Apr 2014.

CrossMark
Click for updates

To cite this article: Ming-Hung Tsai & Jien-Wei Yeh (2014) High-Entropy Alloys: A Critical Review, Materials Research Letters, 2:3, 107-123, DOI: 10.1080/21663831.2014.912690

To link to this article: http://dx.doi.org/10.1080/21663831.2014.912690

PLEASE SCROLL DOWN FOR ARTICLE

Taylor & Francis makes every effort to ensure the accuracy of all the information (the "Content") contained in the publications on our platform. Taylor & Francis, our agents, and our licensors make no representations or warranties whatsoever as to the accuracy, completeness, or suitability for any purpose of the Content. Versions of published Taylor & Francis and Routledge Open articles and Taylor & Francis and Routledge Open Select articles posted to institutional or subject repositories or any other third-party website are without warranty from Taylor & Francis of any kind, either expressed or implied, including, but not limited to, warranties of merchantability, fitness for a particular purpose, or non-infringement. Any opinions and views expressed in this article are the opinions and views of the authors, and are not the views of or endorsed by Taylor & Francis. The accuracy of the Content should not be relied upon and should be independently verified with primary sources of information. Taylor & Francis shall not be liable for any losses, actions, claims, proceedings, demands, costs, expenses, damages, and other liabilities whatsoever or howsoever caused arising directly or indirectly in connection with, in relation to or arising out of the use of the Content.

This article may be used for research, teaching, and private study purposes. Terms & Conditions of access and use can be found at http://www.tandfonline.com/page/terms-and-conditions

It is essential that you check the license status of any given Open and Open Select article to confirm conditions of access and use.

MATERIALS RESEARCH LETTERS

Mater. Res. Lett., 2014
Vol. 2, No. 3, 107–123, http://dx.doi.org/10.1080/21663831.2014.912690

Taylor & Francis
Taylor & Francis Group

www.tandfonline.com/toc/tmrl20/current

High-Entropy Alloys: A Critical Review

Ming-Hung Tsai[a]* and Jien-Wei Yeh[b]*

[a]*Department of Materials Science and Engineering, National Chung Hsing University, Taichung 40227, Taiwan;*
[b]*Department of Materials Science and Engineering, National Tsing Hua University, Hsinchu 30013, Taiwan*

(*Received 10 February 2014; final form 2 April 2014*)

High-entropy alloys (HEAs) are alloys with five or more principal elements. Due to the distinct design concept, these alloys often exhibit unusual properties. Thus, there has been significant interest in these materials, leading to an emerging yet exciting new field. This paper briefly reviews some critical aspects of HEAs, including core effects, phases and crystal structures, mechanical properties, high-temperature properties, structural stabilities, and corrosion behaviors. Current challenges and important future directions are also pointed out.

Keywords: High-Entropy Alloys, High-Entropy Materials, Alloy Design, Mechanical Properties, Corrosion Resistance

Downloaded by [Isfahan University of Technology] at 07:20 25 June 2015

1. Introduction Most conventional alloys are based on one principal element. Different kinds of alloying elements are added to the principal element to improve its properties, forming an alloy family based on the principal element. For example, steel is based on Fe, and aluminum alloys are based on Al. However, the number of elements in the periodic table is limited, thus the alloy families we can develop are also limited. If we think outside the conventional box and design alloys not from one or two 'base' elements, but from multiple elements altogether, what will we get? This new concept, first proposed in 1995,[1] has been named a high-entropy alloy (HEA).[2]

HEAs are defined as alloys with five or more principal elements. Each principal element should have a concentration between 5 and 35 at.%.[2,3] Besides principal elements, HEAs can contain minor elements, each below 5 at.%. These alloys are named 'HEAs' because their liquid or random solid solution states have significantly higher mixing entropies than those in conventional alloys. Thus, the effect of entropy is much more pronounced in HEAs. Existing physical metallurgy knowledge and binary/ternary phase diagrams suggest that such multi-element alloys may develop several dozen kinds of phases and intermetallic compounds, resulting in complex and brittle microstructures that are difficult to analyze and engineer, and probably have very limited practical value. Opposite to these expectations, however, experimental results show that the higher mixing entropy in these alloys facilitates the formation of solid solution phases with simple structures and thus reduces the number of phases. Such characters, made available by the higher entropy, are of paramount importance to the development and application of these alloys. Therefore, these alloys were named as 'high-entropy' alloys.

Because of the unique multiprincipal element composition, HEAs can possess special properties. These include high strength/hardness, outstanding wear resistance, exceptional high-temperature strength, good structural stability, good corrosion and oxidation resistance. Some of these properties are not seen in conventional alloys, making HEAs attractive in many fields. The fact that it can be used at high temperatures broadens its spectrum of applications even further. Moreover, the fabrication of HEAs does not require special processing techniques or equipment, which indicates that the mass production of HEAs can be easily implemented with existing equipment and technologies. More than 30 elements have been used to prepare more than 300 reported HEAs, forming an exciting new field of metallic materials. This paper reviews some crucial aspects of the field, including core effects, phase formation, mechanical properties, high-temperature properties, and corrosion

*Corresponding author. Emails: mhtsai@nchu.edu.tw; jwyeh@mx.nthu.edu.tw

© 2014 The Author(s). Published by Taylor & Francis.
This is an Open Access article distributed under the terms of the Creative Commons Attribution License (http://creativecommons.org/licenses/by/3.0), which permits unrestricted use, distribution, and reproduction in any medium, provided the original work is properly cited. The moral rights of the named author(s) have been asserted.

behaviors. It also points out current challenges and future directions. The physical (magnetic, electrical, and thermal) properties of HEAs have been reviewed elsewhere [4] and are not discussed in this paper.

2. Core Effects [3,5] The multiprincipal-element character of HEAs leads to some important effects that are much less pronounced in conventional alloys. These can be considered as four 'core effects'. This section briefly introduces and discusses the core effects.

2.1. High-Entropy Effect. The high-entropy effect states that the higher mixing entropy (mainly configurational) in HEAs lowers the free energy of solid solution phases and facilitates their formation, particularly at higher temperatures. Due to this enhanced mutual solubility among constituent elements, the number of phases present in HEAs can be evidently reduced. According to $G = H - TS$ (where G is the Gibbs free energy, H is enthalpy, T is temperature, and S is entropy) entropy can stabilize a phase with higher entropy, provided that temperature is sufficiently high. For example, the melting phenomenon of a pure metal is due to the higher entropy of the liquid state relative to the solid state (according to Richard's rule,[6] at melting point the entropy difference between the two states roughly equals the gas constant R). Similarly, among the various types of phases in an alloy, those with higher entropy may also be stabilized at high temperature. In conventional alloys, solid solution phases (including terminal and intermediate solid solutions) have higher mixing entropy than intermetallic compounds do. For HEAs, the difference in entropy between solid solutions and compounds is particularly large owing to the multiprincipal-element design. For example, the configurational entropy of an equimolar quinary random solid solution is $1.61R$. This means that the entropy difference between an equimolar quinary solution and a completely ordered phase (whose entropy is negligible) is about 60% larger than the entropy difference of the melting case mentioned above (i.e. 60% larger than the entropy difference between liquid and solid states of pure metals). Thus, it is highly probable that solid solution phases become the stable phase in HEAs at high temperature. It is expected that with the increase of temperature, the overall degree of order in HEAs decreases. Thus, even those alloys that contain ordered phases in their cast state can transform to random solid solutions at high temperature. However, if the formation enthalpy of an intermetallic compound is high enough to overcome the effect of entropy, that intermetallic compound will still be stable at high temperature.

There is much evidence for the high-entropy effect.[7–13] Here we demonstrate this effect with Figure 1, which shows the XRD patterns of a series of binary to septenary alloys. It is seen that the phases

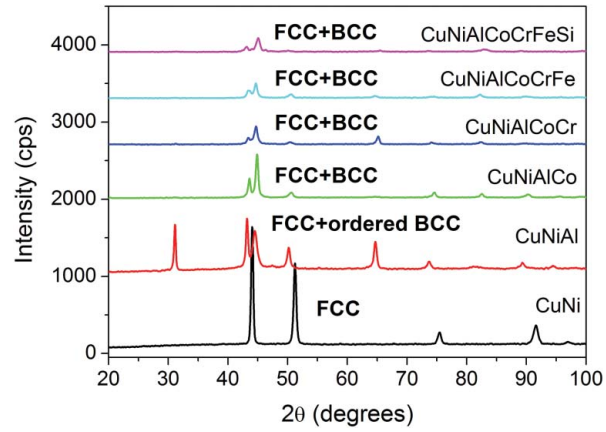

Figure 1. The XRD patterns of a series alloy designed by the sequential addition of one extra element to the previous one. All the alloys have one or two major phases that have simple structures.

in quinary, senary, and septenary alloys remain rather simple: there are only two major phases, and these phases have simple structures such as BCC and FCC (note that the septenary alloy actually contain minor intermetallic phases, although not seen clearly in the XRD pattern). Such simple structures contradict conventional expectation: formation of various kinds of binary/ternary compounds.

Two myths regarding the high-entropy effect are discussed here. The first myth is that the high-entropy effect guarantees the formation of a simple solid solution phase (order/disordered BCC/FCC) at high temperatures. This is not true. Actually, in the very first paper of HEA,[2] the possibility of compound formation was already mentioned. In the same year, the existence of (Cr, Fe)-rich borides in the $AlB_xCoCrCuFeNi$ alloys was observed.[14] As mentioned previously, it is the competition between entropy and enthalpy that determines the phase formation. The large negative formation enthalpy of the borides thus justifies their stability at high temperatures. Similar phenomena have also been observed in other high-temperature annealing experiments.[15–17] The second myth is that only simple solid solution phases (BCC/FCC) are the desired phases for practical applications of HEAs. This is also not true. It is true that these multiprincipal-element simple solid solution phases are unique to HEAs, and they can have outstanding properties. However, as shown later, many HEAs containing intermediate phases also have great potential. Thus, the exploration of HEAs should not be limited to simple solid solution phases.

2.2. Sluggish Diffusion Effect. It was proposed that the diffusion and phase transformation kinetics in HEAs are slower than those in their conventional counterparts.[18] This can be understood from two

Downloaded by [Isfahan University of Technology] at 07:20 25 June 2015

Downloaded by [Isfahan University of Technology] at 07:20 25 June 2015

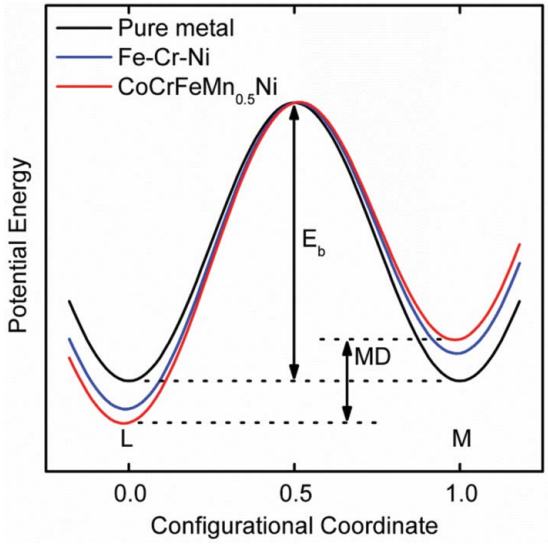

Figure 2. Schematic diagram of the potential energy change during the migration of a Ni atom. The mean difference (MD) in potential energy after each migration for pure metals is zero, whereas that for HEA is the largest.[19]

aspects. Firstly, in HEA the neighboring atoms of each lattice site are somewhat different. Thus, the neighbors before and after an atom jump into a vacancy are different. The difference in local atomic configuration leads to different bonding and therefore different local energies for each site. When an atom jumps into a low-energy site, it becomes 'trapped' and the chance to jump out of that site will be lower. In contrast, if the site is a high-energy site, then the atom has a higher chance to hop back to its original site. Either of these scenarios slows down the diffusion process. Note that in conventional alloys with a low solute concentration, the local atomic configuration before and after jumping into a vacancy is, most of the time, identical. Tsai et al. used a seven-bond model to calculate the effect of local energy fluctuation on diffusion.[19] They showed that for Ni atoms diffusing in Co–Cr–Fe–Mn–Ni alloys (which has a single-phase, FCC structure), the mean potential energy difference between lattice sites is 60.3 meV, which is 50% higher than that in Fe–Cr–Ni alloys (see Figure 2). This energy difference leads to a significantly longer occupation time at low-energy sites (1.73 times longer than that at high-energy sites). Indeed, diffusion couple experiments show that the activation energy of diffusion in the Co–Cr–Fe–Mn–Ni alloys is higher than those in other FCC ternary alloys and pure elements (Table 1).[19] The diffusivity of Ni at the respective melting point of each metal is also calculated (Table 1). The slowest diffusion takes place again in the Co–Cr–Fe–Mn–Ni alloys.

Secondly, the diffusion rate of each element in a HEA is different. Some elements are less active (for example, elements with high melting points) than others so these elements have lower success rates for jumping into vacancies when in competition with other elements. However, phase transformations typically require the coordinated diffusion of many kinds of elements. For example, the nucleation and growth of a new phase require the redistribution of all elements to reach the desired composition. Grain growth also requires the cooperation of all elements so that grain boundaries can successfully migrate. In these scenarios, the slow-moving elements become the rate-limiting factor that impedes the transformation.

The slow kinetics in HEAs allows readily attainable supersaturated state and nano-sized precipitates, even in the cast state.[2,20,21] It also contributes to the excellent performance of HEA coatings as diffusion barriers.[22, 23] Moreover, it allows better high-temperature strength and structural stability, which are discussed in Section 5. For the same reason, HEAs are also expected to have outstanding creep resistance.

2.3. Severe-Lattice-Distortion Effect. The lattice in HEAs is composed of many kinds of elements, each with different size. These size differences inevitably lead to distortion of the lattice. Larger atoms push away their neighbors and small ones have extra space around. The strain energy associated with lattice distortion raises the overall free energy of the HEA lattice. It also affects the properties of HEAs. For example, lattice distortion impedes dislocation movement and leads to pronounced

Table 1. Diffusion parameters for Ni in different FCC matrices. The compositions of Fe-Cr-Ni(-Si) alloys are in wt.%.[19]

Solute	System	D_0 (10^{-4} m^2/s)	Q (kJ/mol)	$T_m(T_s)$ (K)	Q/T_m	D_{T_m} (10^{-13} m^2/s)
Ni	CoCrFeMnNi	19.7	317.5	1607	0.1975	0.95
	FCC Fe	3	314	1812	0.1733	2.66
	Co	0.43	282.2	1768	0.1596	1.98
	Ni	1.77	285.3	1728	0.1651	4.21
	Fe-15Cr-20Ni	1.5	300	1731	0.1733	1.33
	Fe-15Cr-45Ni	1.8	293	1697	0.1727	1.73
	Fe-22Cr-45Ni	1.1	291	1688	0.1724	1.09
	Fe-15Cr-20Ni-Si	4.8	310	1705	0.1818	1.53

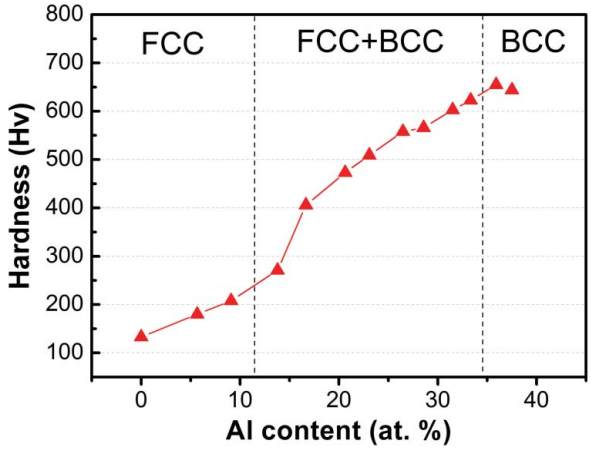

Figure 3. Hardness of the $Al_xCoCrCuFeNi$ alloys as a function of Al content.

solid solution strengthening (see Section 4.4). It also leads to increased scattering of propagating electrons and phonons, which translates to lower electrical and thermal conductivity.[4]

2.4. Cocktail Effect. The properties of HEAs are certainly related to the properties of its composing elements. For example, addition of light elements decreases the density of the alloy. However, besides the properties of the individual composing elements, the *interaction* among the component elements should also be considered. For example, Al is a soft and low-melting-point element. Addition of Al, however, can actually harden HEAs. Figure 3 plots the hardness of the $Al_xCoCrCuFeNi$ alloy as a function of Al content. It is clearly seen that the alloy hardens significantly with the addition of Al. This is partly because of the formation of a hard BCC phase, and partly due to the stronger cohesive bonding between Al and other elements, and its larger atomic size. Thus, the macroscopic properties of HEA not only come from the averaged properties of the component elements, but also include the effects from the excess quantities produced by inter-elemental reactions and lattice distortion.

3. Phase and Crystal Structure In conventional alloys, phases are typically classified into three types: terminal solutions, intermediate solutions, and intermetallic compounds. We can use similar, but expanded concepts to classify phases in HEAs. *Terminal phases* are phases based on one dominating element. The definition of *intermetallic compounds* is not changed: they are stoichiometric and have fixed composition ratio. However, because phases in HEAs typically have a composition range rather than fixed composition ratio, intermetallic compounds are rarely seen in HEAs. *Solution phases* are phases not belonging to the above two categories. This category includes the solid solutions based on both simple (e.g. BCC and FCC) and complex structures (e.g. Laves phase).

In the literature, phases in HEAs are usually classified differently. They are often classified as: random solid solution (e.g. FCC, BCC), ordered solid solution (e.g. B2 and $L1_2$), and intermetallic phases (e.g. Laves phases). This classification may lead to some confusion because by definition, intermetallic phases can also be classified as ordered solid solutions—they have composition ranges and are typically ordered. In view of this, we suggest classifying the phases according to their structure (simple/complex) and ordering (ordered/disordered). A phase is said to be *simple* if its structure is identical to or derived from FCC, BCC or HCP structures. Namely, cI2-W, cF4-Cu, and hP2-Mg structures and their ordered versions (superlattices) such as cP2-CsCl (B2) and cP4-AuCu3 ($L1_2$) structures are simple.[24] If a phase is not simple (e.g. Laves phases), it is said to be *complex*. Therefore, the above three types now becomes: simple disordered phase (SDP), simple ordered phase (SOP), and complex ordered phase (COP).

3.1. Simple Solid Solution or Intermetallics?. One fundamental and important question regarding HEAs is: what kind of phase and crystal structure will form when we mix so many different elements together? To the surprise of most people, simple structures (SDPs and SOPs) are the most frequently seen in as-cast HEAs (see Figure 1). These simple phases originate from the high-entropy effect mentioned previously. Besides simple phases, different kinds of COPs, such as σ, μ, Laves, etc., are also observed in HEAs. Because simple-solution phases with more than five elements are unique to HEAs, researchers have worked intensely to understand the conditions for their formation.

From the classic Hume-Rothery rules, factors that affect the formation of binary solid solutions include atomic size difference, electron concentration, and difference in electronegativity.[25] Besides these factors, enthalpy and entropy of mixing are the most important phase formation parameters for HEAs. Zhang et al. [26] and Guo et al. [27] studied the effect of these parameters on the phase formation of HEAs and obtained similar conclusions: the formation of simple or complex phases depends mainly on the enthalpy of mixing (ΔH_{mix}), entropy of mixing (ΔS_{mix}), and atomic size differences (δ). In order to form sole simple phases (i.e. FCC, BCC, and their mixtures, including both ordered/disordered cases), the following conditions have to be met simultaneously: $-22 \leq \Delta H_{mix} \leq 7\,\text{kJ/mol}$, $\delta \leq 8.5$, and $11 \leq \Delta S_{mix} \leq 19.5\,\text{J/(K mol)}$.[27] This is shown in Figure 4, where the boundary of simple phases is shown. These conditions are quite logical: ΔH_{mix} cannot be too large in value because large positive ΔH_{mix} leads to phase separation and large negative ΔH_{mix} typically leads to

Downloaded by [Isfahan University of Technology] at 07:20 25 June 2015

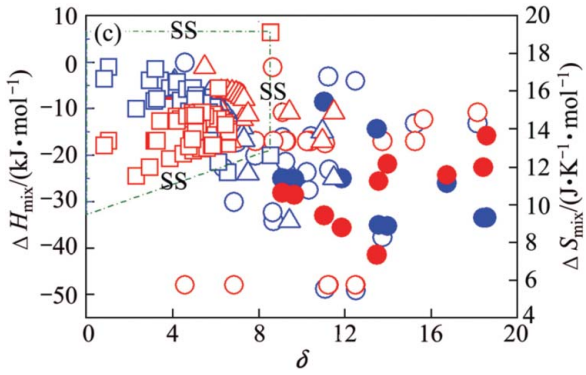

Figure 4. Superimposed effect of ΔH_{mix}, δ, and ΔS_{mix} on phase stability in equiatomic multicomponent alloys and BMGs. Notes: Blue symbols indicate the relationship between ΔH_{mix} and δ, while red ones represents that between ΔS_{mix} and δ. Symbol ○ represents equiatomic amorphous phase-forming alloys; ● represents nonequiatomic amorphous phase-forming alloys; □ represents simple phases and △ represents intermetallic phases. The region delineated by the dash-dotted lines indicates the requirements for simple phases to form.[27]

intermetallic phases. δ has to be small enough since large δ leads to excess strain energy and destabilizes simple structures. ΔS_{mix} has to be large enough because it is the main stabilizing factor for simple phases. If the target of discussion is limited to SDPs only, the conditions are more strict: $-15 \leq \Delta H_{mix} \leq 5$ kJ/mol, $\delta \leq 4.3$, and $12 \leq \Delta S_{mix} \leq 17.5$ J/(K mol).[26]

The other criterion to judge whether or not sole simple phases will form in an HEA is the parameter $\varepsilon = |T\Delta S_{mix}/\Delta H_{mix}|$.[28,29] Based on the concept of entropy–enthalpy competition (see Section 2.1), ε represents the effect of entropy relative to that of enthalpy. Thus, larger ε suggests a higher possibility of forming SDP, which agrees well with the analysis.[28,29] A drawback of the two criterions shown above is that even if an alloy is designed following these criterions, it can still contain intermetallic phases. This can be seen in Figure 4. The 'solid solution' region delineated by the dash-dotted lines still contains triangles, indicating the existence of intermetallic phases. A new thermodynamic parameter has been proposed to solve this problem, and the results will be published soon.[30]

Some points of notice should be mentioned here: Firstly, the above analyses are based on the as-cast state. This is natural because most reported HEAs are in their as-cast state. Secondly, the phases observed macroscopically in as-cast HEAs can contain atomic-scale decompositions/inhomogeneities. This is evidenced by detailed transmission electron microscopy (TEM) and atomic probe analysis.[21,31,32] Thirdly, in HEAs similar disordered and ordered versions of the same base structure often co-exist.[8,33–35] For example, coexistence of BCC and ordered BCC (B2) phases was frequently reported.[8,21,34] Coexistence of FCC and ordered FCC ($L1_2$) phases was also observed.[35] When these phases have nearly identical lattice parameter, their XRD peaks overlap (except the superlattice peaks). Therefore, when the amount of the SOP is small, XRD may reflect only the peaks belonging to SDP, even if SOP exists.[34,35] This indicates that TEM analysis is needed to really confirm the existence of SOP.[34,35]

3.2. Crystal Structure of Simple Solid Solution Phases.

If an HEA does crystallize into simple phases, what will the structure of the phase be? Virtually all simple solid solution phase observed in HEAs have either BCC or FCC structures.[8,10,36,37] The most critical factor that decides whether an alloy crystallizes into BCC or FCC structure appears to be its VEC (valence electron concentration, the VEC of an alloy is calculated from the

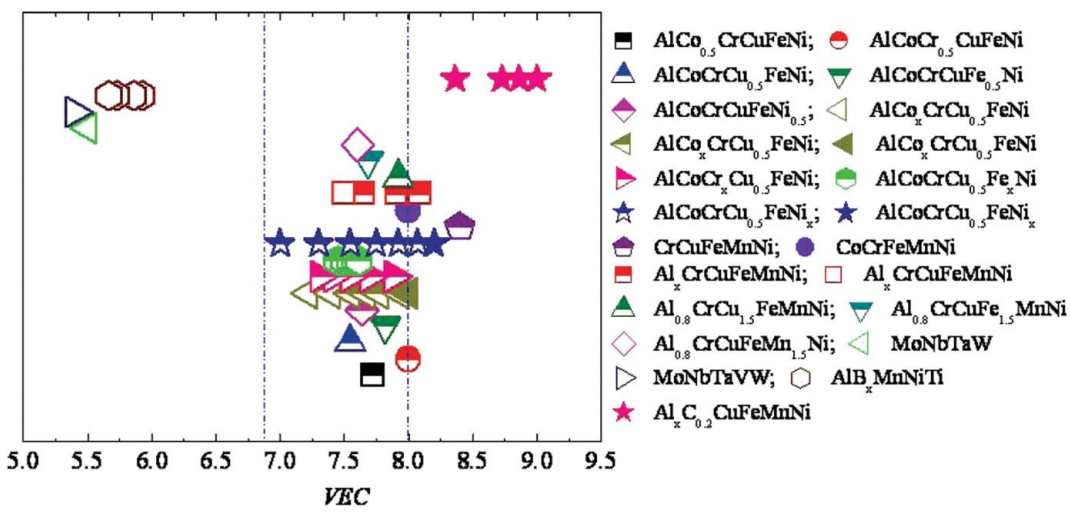

Figure 5. Relationship between VEC and the FCC, BCC phase stability for various HEA systems. Notes: Fully closed symbols for sole FCC phases; fully open symbols for sole BCC phase; top-half closed symbols for mixed FCC and BCC phases.[38]

Downloaded by [Isfahan University of Technology] at 07:20 25 June 2015

Downloaded by [Isfahan University of Technology] at 07:20 25 June 2015

weighted average VEC of the constituent components). Guo et al. summarized the relationship between VEC and structure of many HEAs (Figure 5).[38] They found that when the VEC of the alloy is larger than 8, the FCC structure is stabilized. When the VEC of the alloy is smaller than 6.87, the BCC structure is stabilized. Co-existence of FCC and BCC phase is observed at VEC values between 6.87 and 8.[38] However, the mechanism behind the effect of VEC on phase formation has not been fully understood so far.

3.3. High-Entropy Bulk Metallic Glass. Although HEAs and bulk metallic glasses (BMGs) are both multi-component and their compositions look similar at first glance, these two classes of materials are based on completely different concepts. For HEAs, more than five principal elements are required. In contrast, most BMGs are based on one or two principal elements. More importantly, BMGs are characterized by their amorphous structure, but there is no structural requirement for HEAs. The concept of HEAs, however, triggered an idea: would there be good glass formers in HEAs? If so, how do we design high-entropy BMGs (HEBMGs) with good glass-forming ability (GFA) and better properties?

Inoue's empirical rules [39] state that (1) more than three composing element, (2) large atomic size differences, and (3) large negative mixing enthalpies favor the formation of BMGs. The first rule is in line with the design concept of HEAs. Indeed, high configurational entropy in HEAs was found to be beneficial for glass formation. This was evidenced by lower critical cooling rates in BMGs with higher ΔS_{mix}.[27] Another earlier study also reported similar findings.[40] The second and third rules for BMG formation are exactly opposite to the requirements to form simple phases in HEAs (see Section 3.1). This suggests that one should choose HEAs that are predicted to form intermetallic phases rather than simple phases as candidates for HEBMGs. Indeed, very recently Guo et al. analyzed the ΔH_{mix} and δ of some HEAs and BMGs and found that simple-solution-type HEAs and BMGs fall in opposite corners of the δ-ΔH_{mix} plot (shown in Figure 6 [41]). They further pointed out that as long as the competition from intermetallic phases can be ruled out by composition adjustment, HEAs that locate in the amorphous phase region of the δ-ΔH_{mix} plot indeed solidify into metallic glasses.[41] This strategy has been successfully demonstrated in a series of Zr-containing alloys prepared via melt spinning.[41]

Not many HEBMGs have been fabricated till now. Most of these HEBMGs have diameters smaller than 3 mm.[42–46] Takeuchi et al. successfully prepared $Pd_{20}Pt_{20}Cu_{20}Ni_{20}P_{20}$ HEBMG with a maximum diameter of 10 mm.[47] But they suggested that conventional GFA assessment parameters such as T_{rg} (reduced glass transition temperature normalized with liquidus temperature) cannot evaluate the GFA of HEBMG effectively. Other factors, e.g. Gibbs free energy assessments, need to be taken into account.[47] Apparently more study is needed to understand these issues.

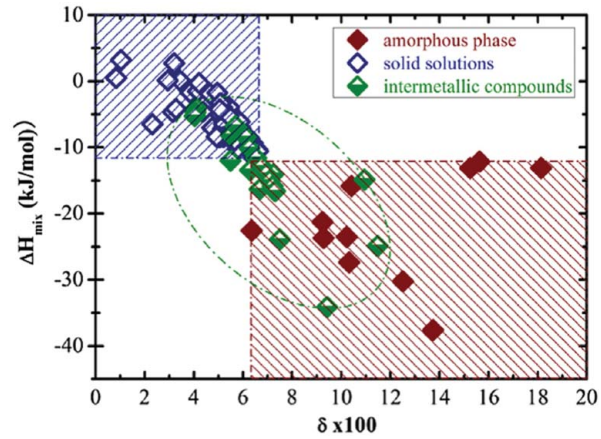

Figure 6. The δ-ΔH_{mix} plot delineating the phase selection in HEAs. Note: The dash-dotted regions highlight the individual region to form simple solid solutions, intermetallic phases and amorphous phases.[41]

The distinct composition design in HEAs brings with their amorphous structure other special properties. For example, an extremely high crystallization temperature (probably the highest among reported BMG) of over 800°C and good performance as diffusion barrier between Cu and Si was observed in 20-nm-thick NbSiTaTiZr alloy film.[23] Additionally, $Zn_{20}Ca_{20}Sr_{20}Yb_{20}(Li_{0.55}Mg_{0.45})_{20}$ shows room temperature homogeneous flow and a plasticity of 25%,[44] which is in sharp contrast to the typical shear banding and brittle behavior of most BMGs. Very recently CaMgZnSrYb, a high-entropy modification of $Ca_{65}Mg_{15}Zn_{20}$ BMG, has shown improved properties in orthopedic applications.[48] CaMgZnSrYb not only has better mechanical properties, but also promotes osteogenesis and new bone formation after two weeks of implantation. These examples indicate that high-entropy BMGs and amorphous films do have great potential and deserve further exploration—which is good news for both communities.

3.4. Phases at Elevated Temperatures. As mentioned in Section 3.1, our understanding of the phases in HEAs focuses mainly on their as-cast state. However, the cast state is typically not in thermodynamic equilibrium. For alloys that locate in the BCC or FCC phase region suggested by Guo et al. (see Figure 5 [38]), phase transformation may be less significant. For example, no phase formation was found in the Co–Cr–Fe–Mn–Ni FCC alloys during their high-temperature annealing.[14,17] For alloys that locate in the BCC+FCC phase region,

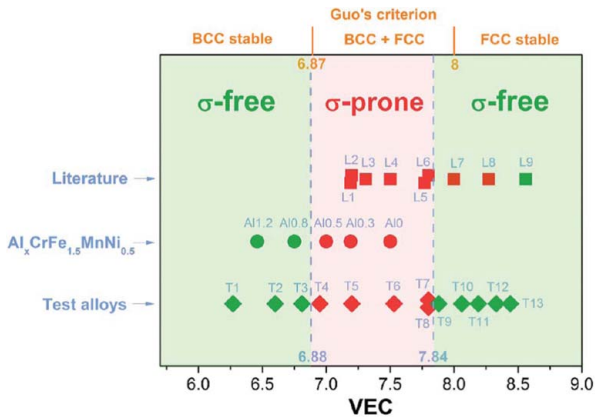

Figure 7. Relationship between the VEC and the presence of σ phase after aging for a number of HEAs. Green and red icons indicate the absence and presence of σ phase after aging, respectively.[52]

however, phase transformation will take place at higher temperatures. In the Al-Co-Cr-Cu-Fe-Ni system, annealing at ~800°C or below increases the fraction of the BCC phase.[49] Annealing at temperatures higher than 800°C increases the fraction of the FCC phase. Because the FCC phase is ductile and the BCC phase is relatively brittle, annealing can be used to tune the mechanical properties.

Some alloys have phases that are stable at intermediate temperatures only. These alloys may contain only simple phases in their as-cast state due to the higher cooling rate of Cu mold casting. Upon annealing, however, the intermediate-temperature phases will appear. For example, η phase [17,50] and σ phase [12,34,51] are known to form in some HEAs. One should pay great attention to the formation of these intermediate-temperature phases, because their formation can lead to significant changes in mechanical properties. Tsai et al. studied the stability of the σ phase.[52] They showed that the formation of the σ phase is predictable: it is directly related to the VEC of the alloy. As shown in Figure 7,[52] there is a σ-phase-forming VEC range for HEAs based on Al, Co, Cr, Cu, Fe, Mn, Ni, Ti, and V. Alloys whose VEC fall in this range develop σ phase upon annealing at 700°C.

3.5. Computer-Aided Phase Prediction. The multi-principal-element nature of HEA translates to an immense amount of possible compositions. It takes huge amounts of time and cost to study all the compositions experimentally. Hence, it is critically important to implement highly efficient, low-cost methods to assist experimental study. For example, phase diagram is one of the most important tools to understand an alloy system. However, developing the phase diagram of just one senary HEA requires tremendous efforts—there are six composition axes! If the phase diagram could be reliably predicted with computational techniques, then experiments are only needed to verify some critical points on the predicted phase diagram, and the work needed is significantly reduced.

The main problem in applying existing phase-prediction techniques (e.g. CALculation of PHAse Diagrams, CALPHAD) on HEAs is probably the lack of a suitable database for multicomponent systems.[53] Thus, Zhang et al. developed a thermodynamic database for the Al–Co–Cr–Fe–Ni alloy system by extrapolating binary and ternary systems to wider composition ranges.[53] This database does not consider quaternary or quinary interaction parameters. Using their database, they obtained phase diagrams of the Al–Co–Cr–Fe–Ni system that agree with available experimental results.

In some cases, it seems that phase diagrams with reasonable accuracy can still be obtained even without the development of new databases. An Ni-based superalloy database was used to predict the equilibrium phases and phase fractions of $Al_{0.5}CoCrCuFeNi$, $Al_{23}Co_{15}Cr_{23}Cu_8Fe_{15}Ni_{16}$ and $Al_8Co_{17}Cr_{17}Cu_8Fe_{17}Ni_{33}$ alloys.[12,31] Except for some minor discrepancies,[12] experiments and predictions agree with each other. These examples demonstrate the effectiveness of computational methods in predicting the phase of HEAs. Although the accuracy of computational phase predictions for other HEA systems (other than Al–Co–Cr–Cu–Fe–Ni) is still not clear (the only result appears to be not as pleasing [54]), it is greatly expected that these techniques will become important tools for the future design and development of HEAs.

3.6. Phase Evolutions in Representative Alloy Systems. The phase evolutions in some important alloy systems are discussed, along with their mechanical properties, in Sections 4.2 and 4.3. This is because the mechanical properties of HEAs are directly related to the phases contained in the alloys (see Section 4.1). Therefore, the best way to understand the mechanical properties is to discuss phase evolution and mechanical properties together.

4. Mechanical Properties

4.1. Basic Concepts and Deformation Behaviors. Because of the wide composition range and the enormous number of alloy systems in HEAs, the mechanical properties of HEA can vary significantly. In terms of hardness/strength, the most critical factors are:

(1) Hardness/strength of each composing phase in the alloy;
(2) Relative volume ratio of each composing phase;
(3) Morphology/distribution of the composing phases.

Downloaded by [Isfahan University of Technology] at 07:20 25 June 2015

Table 2. Phases in HEAs as categorized by hardness. Examples and typical hardness range for each category are also listed.

Type	Examples	Typical hardness (HV)
Valence compounds	Carbides, borides, silicides	1000–4000
Intermetallic phases with non-simple structures	σ, Laves, η	650–1300
BCC and derivatives	BCC, B2, Heusler	300–700
FCC and derivatives	FCC, $L1_2$, $L1_0$	100–300

The first factor is largely determined by the crystal structure and bonding of each phase. In our experience, the phases can be roughly classified into four categories each having a different hardness range. This is provided in Table 2. It is important to note that the hardness ranges listed in Table 2 are merely typical ranges and there could be exceptions. Valence compounds are based on very strong covalent bonding and are essentially ceramics. Thus, their hardness is the highest. Non-simple intermetallic phases often lack easily accessible slip systems and dislocation activities are thus largely hindered. BCC and BCC-derivative structures (see the second paragraph of Section 3) are harder than their FCC counterparts because BCC-based structures have stronger directional bonding and lack a truly close-packed slip plane.[55,56]

The general rule to estimate the hardness/strength of an HEA is straight forward: the harder the phase (and the higher the fraction of the hard phase), the harder the alloy. When two HEAs have phases with similar hardness and relative fraction, the distribution of the phases can also play an important role. This is exemplified in later sections. The ductility of HEA is also related to the phase in the alloy. As can be expected, harder phases usually have lower ductility.

The deformation microstructure and mechanism in most HEAs is unclear. However, such information was revealed in a single-phase, FCC CoCrFeMnNi alloy via detailed TEM study.[57] It was found that at small strains (<2.4%), the deformation is governed by planar slip of $1/2\langle 110\rangle$ type dislocations on $\{111\}$ planes. At a strain around 20%, the deformation behavior depends on the deformation temperature. At 77 K, higher strain leads to the prevalence of deformation twinning. At 293 K, however, higher strain leads to the formation of dislocation cell structures. The texture evolution (during cold rolling) and recrystallization behavior in the same alloy have also been studied.[58] The texture after 90% cold rolling was predominantly brass-type, which indicates low stacking fault energy (SFE). Bhattacharjee et al. suggested that the lower SFE in HEAs is due to the higher free energy of the 'perfect crystal' in HEAs. This is explained in further detail in the last paragraph of Section 5. The recrystallization texture in the CoCrFeMnNi alloy retains components from previous cold rolling, which is similar to low-SFE TWIP steels and 316 stainless steel. However, the relative proportions of various texture components between HEA and other low-SFE alloys are different. The main reasons are the slower recrystallization rate in regions with brass texture, and the absence of preferential nucleation of brass-textured grains from shear bands.[58] The low SFE in the CoCrFeMnNi alloy as suggested by Bhattacharjee et al. [58] is indeed confirmed by Zaddach et al.[59] They combined experiments with first-principle calculations and concluded that the SFE of CoCrFeMnNi is between 18.3 and 27.3 mJ/m^2. This value is close to that of conventional low-SFE alloys such as AISI 304L and brass.

The cold deformation and annealing behaviors of another FCC-based HEA, the $Al_{0.5}CoCrCuFeNi$ alloy, was also investigated.[60] Deformation twinning is observed again in this alloy. Prevalence of twinning appears to result from the blockage of local slip by the Widmanstätten precipitates. The above results suggest that in FCC HEAs, dislocation slip and twinning are still the main deformation mechanisms.

4.2. The Al-Co-Cr-Cu-Fe-Ni Alloy System. Of all the HEA systems reported, Al-Co-Cr-Cu-Fe-Ni [7,8,21,35,36,49,60–68] and its Cu-free version Al-Co-Cr-Fe-Ni [69–74] have been studied most comprehensively. Most of the reported HEA systems emerge from them. The main difference between the two is the presence of Cu-rich interdendrite in the former. This is because Cu has positive mixing enthalpies with most of the other elements, and is thus repelled to the interdendrite region. Additionally, remnant Cu in the dendrite region also clusters and forms various kinds of precipitates.[21,35,60] The main phases in cast Al-Co-Cr-Cu-Fe-Ni alloy include FCC, BCC/B2, and the Cu-rich phase (also has an FCC structure). The relative volume ratio of these phases depends on the composition. The relative volume of BCC and FCC phases is related to the VEC of the alloy. Higher VEC typically leads to more of the FCC phase, and vice versa. Al has the strongest effect in this regard,[36] and addition of Al leads to the transition of the FCC phase to the BCC phase. Additionally, when there is sufficient Al, BCC tend to further decompose to a (Al, Ni)-rich B2 phase and a (Cr, Fe)-rich BCC phase that have almost identical lattice parameters.[8,21,71,74] The Cu-rich phase appears clearly when the concentration of Cu is higher than ~10 at.%. Its fraction increases with the content of Cu. In general, hardness of the FCC phase is

Downloaded by [Isfahan University of Technology] at 07:20 25 June 2015

Downloaded by [Isfahan University of Technology] at 07:20 25 June 2015

between HV 100–200.[7,8,70–72] Alloys having a sole FCC phase have ductilities between 20–60%, and usually exhibit significant work hardening.[62,63,69] Hardness of the BCC/B2 phase is typically between HV 500–600. Because addition of Al triggers the formation of hard BCC/B2 phase, and hardness of the alloy increases with Al content [7,8,70–72] (see Figure 3). Alloys having sole BCC/B2 phases probably have ductilities less than 5%.[62] In terms of their plasticity, values of 30% or higher have been reported.[74] Superplasticity was observed in AlCoCrCuFeNi at 800–1000°C, and the elongation was between 405 and 800%.[65]

Effect of annealing on the mechanical properties of the Al-Co-Cr-Cu-Fe-Ni system depends on the phase transformation involved (see Section 3.4). When the selected annealing temperature favors the formation of BCC phase, the alloy becomes harder and more brittle. When the temperature selected increases the fraction of FCC phase, the alloys softens and becomes more ductile. It should be carefully noted that in this alloy system, a long annealing time may lead to the formation of σ phase,[12] which hardens the alloy but remarkably reduces its ductility/plasticity.[12,34,51]

4.3. Derivatives of the Al-Co-Cr-Cu-Fe-Ni Alloy System. This section discusses the mechanical properties of alloys derived from the Al-Co-Cr-Cu-Fe-Ni system. A system is said to be 'derived' from Al-Co-Cr-Cu-Fe-Ni when the number of different principal element between the two systems is less than two. For example, Al-Co-Cr-Cu-Ti is derived from Al-Co-Cr-Cu-Fe-Ni (replace Fe with Ti and remove Ni).

Addition of Ti to Al-Co-Cr-Cu-Fe-Ni usually leads to formation of intermetallic phases such as the Laves phase,[15,75–79] σ phase,[17,75,76] Heusler phase,[17] η-Ni_3Ti,[17,50] and R phase.[76] This is because Ti has large negative enthalpy of mixing with rest of the composition. These phases strengthen the alloy. For example, $AlCoCrFeNiTi_{0.5}$ has a high yield strength of 2.26 GPa and a plasticity of 23% (Figure 8).[77] The hardness of $Al_{0.5}CoCrCuFeNiTi_x$ alloy can be significantly increased to HV 600 or higher when x is larger than 1.[75] The hardness of Ti-containing alloys may further increase upon annealing owing to the formation of more intermetallic phases.[17,50]

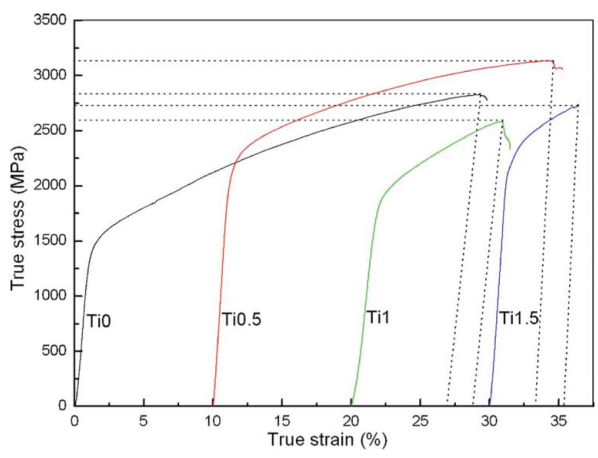

Figure 8. Compressive true stress-strain curves of $AlCoCrCuFeNiTi_x$ alloys with x being 0, 0.5, 1, and 1.5.[77]

Addition of Mo to the system generally leads to the formation of (Cr, Mo, Co, Fe)-rich σ phase.[80–87] σ phase is a very hard and brittle intermetallic phase. As mentioned previously, it significantly enhances the hardness of the alloy but reduces its ductility/plasticity. For example, addition of 0.5 mole fraction of Mo to AlCoCrFeNi raises its strength from 1,051 to 2,757 MPa.[86]

Addition of Mn leads to two representative systems, the CoCrFeMnNi and $Al_xCrFe_{1.5}MnNi_{0.5}$ alloys. The CoCrFeMnNi alloy is a classic sole-FCC HEA and does not experience phase transformation when annealed. Therefore, it is a good model system to study the behavior of multiprincipal-element solid solutions and has been used to study the grain growth,[88] diffusion,[19] dislocation behavior,[57] and texture evolution [58] of FCC HEAs. This alloy is soft (yield strength ~170 MPa), very ductile (elongation ~60%), and shows high strain hardening capability at room temperature. At 77 K, its strength nearly doubles and its elongation increases to ~80%.[57] The $Al_{0.3}CrFe_{1.5}MnNi_{0.5}$ alloy is a representative age-hardening HEA. When aged between 600 and 900°C, its hardness boosts from about 300 HV to almost 900 HV.[34,51,89] TEM observation shows that the hardening phenomenon is not from precipitation hardening, but from the transformation of the BCC matrix to the σ phase during aging.[34] The hardening phenomenon in this alloy can actually be controlled to occur only near the surface, forming a surface hardening layer that significantly improves wear resistance (see Section 4.5).

Addition of non-metallic elements such as Si and B leads to the formation of valence compounds such as silicides and borides. These compounds also lead to evident hardening. For example, the hardness of AlCoCrFeNi**Si** [90] and Al**B**CoCrCuFeNi [14] are HV 738 and HV 740, respectively. Compound formation also causes loss of toughness. Addition of Si to AlCoCrFeNi by the equimolar ratio reduces its plastic strain from over 25% to ~1%.[90] It should be noted that although valence compounds are typically harder than intermetallic phases, silicide/boride-containing alloys are not necessarily harder than alloys containing intermetallic phase. In the two alloys mentioned above (AlCoCrFeNi**Si** and Al**B**CoCrCuFeNi), the volume fractions of silicides and borides are not high, and the distribution of these compounds is quite localized. Hard phases with such morphology (isolated coarse laths) are less effective in

Downloaded by [Isfahan University of Technology] at 07:20 25 June 2015

strengthening, particularly when they are embedded in an apparently softer matrix. Besides the above, many other elements have been added to the Al-Co-Cr-Cu-Fe-Ni system (e.g. Zr [91], Nd [91], Nb [92], V [93,94], Y [95], Sn [96,97], Zn [98], and C [99,100]).

4.4. Refractory HEA systems. Some researchers developed HEAs that are based on totally different elements. The most notable system is the refractory HEA system developed by Senkov et al.[10,37,54,101–106] These alloys are composed mainly of refractory elements such as Cr, Hf, Mo, Nb, Ta, V, W, and Zr. The major phase in these alloys is typically BCC. Many of them even have a sole BCC structure. These BCC solid solutions have high strength ranging from 900 to 1,350 MPa.[37,101,105,106] Interestingly, such strength is several times higher than that of the weighted average strength of the composing elements. For example, the rule-of-mixture hardness of MoNbTaVW and HfNbTaTiZr are 1,596 and 1,165 MPa, respectively. However, the hardness measured for these alloys are more than three times higher: 5,250 and 3,826 MPa, respectively. Such high hardness is a result of the solid solution strengthening effect which originated from the difference in atomic size and modulus among the composing elements.[37] Room temperature plasticity of refractory HEA is closely related to composition. The plastic fracture strain is less than 5% for many alloys. However, some alloys can be compressed to 50% without fracture.[37,103,106] It was suggested that the high plasticity in some alloys is owing to the prevalence of deformation twinning.[37,103] It is worth mentioning that refractory HEAs can show superb mechanical properties at elevated temperatures, which is described in Section 5.

4.5. Wear and Fatigue Properties. Wear properties of HEAs, under both abrasive [7,14,51,75,94,107] and adhesive [50,66,80] conditions, have been tested in a number of systems. The adhesive wear properties of tested HEAs are summarized in Figure 9. HEAs composed solely of SDPs typically do not show better wear properties than conventional alloys with similar hardness (e.g. compare $Al_{0.5}CoCrCuFeNi$ and 316SS in Figure 9). Wear resistance is clearly enhanced in the presence of some B2 or COPs (e.g. $Al_2CoCrCuFeNi$ and $AlCoCrFe_{1.5}Mo_{0.5}Ni$). If COPs with high hardness become the main phase, wear resistance is often outstanding. Many HEA systems of this type have comparable or even better performances than conventional wear-resistant alloys such as SKD61 tool steel (AISI H13) and SUJ2 bearing steel (AISI 52100).[50,51,80,107] For example, the wear resistance of the $AlCoCrFeMo_{0.5}Ni$ alloy is comparable to that of SUJ2 (Figure 9). In particular, the $Al_{0.2}Co_{1.5}CrFeNi_{1.5}Ti$ alloy [50] has significantly

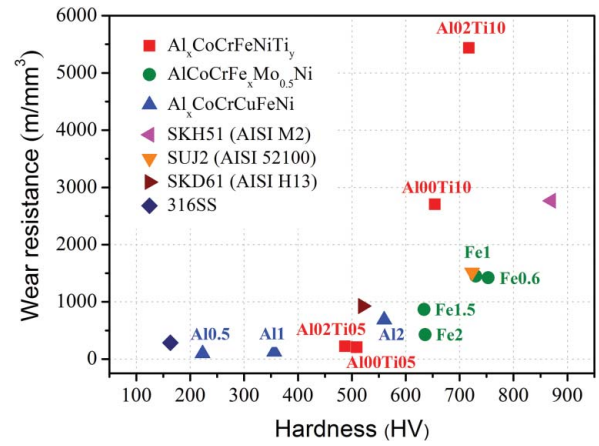

Figure 9. Relationship between hardness and adhesive wear resistances of various HEAs and conventional alloys.[50,66,80]

better wear resistance than SUJ2 and SKH51 (AISI M2, see Figure 9). Its hardness is similar to that of SUJ2, but its wear resistance is 3.6 times that of the latter. The wear resistance of the $Al_{0.2}Co_{1.5}CrFeNi_{1.5}Ti$ alloy is twice that of SKH51, but the hardness of the latter is a lot higher. The outstanding performance is owing to the higher hardness of HEA at high temperatures. Additionally, because the wear mechanism is mild oxidational wear, the better oxidation resistance in the $Al_{0.2}Co_{1.5}CrFeNi_{1.5}Ti$ alloy is also beneficial to its wear resistance.[50]

The $Al_{0.3}CrFe_{1.5}MnNi_{0.5}$ alloy (see also Section 4.3) has a unique surface hardening phenomenon that can increase its wear resistance by ~50%, but only reduce its bending strain by 2%. This is achieved by limiting the formation of hard σ phase at the surface region. Because the heterogeneous nucleation energy and strain energy near the free surface are lower than those in the interior of the alloy, one can carefully select the aging temperature so that the kinetics of the transformation is sufficient high only at the near-surface region. The process is simple (atmospheric aging), applicable to objects with complex shapes, and offers a markedly better combination of mechanical properties than SUJ2 (30% higher wear resistance and 300% larger maximum bending strain).

Preliminary fatigue results are also encouraging. $Al_{0.5}CoCrCuFeNi$ alloy can show long fatigue lives at relatively high stresses, high endurance limits (540–945 MPa) and endurance limit to ultimate tensile strength ratio (0.402–0.703).[67] These values are comparable to or even better than many conventional alloys, such as various steels, Ti alloys, and Zr-based BMGs.[67] Although some degree of scattering in fatigue life was observed, it is probably due to defects introduced during sample preparation. If defects can be carefully controlled, the fatigue resistance characteristics in $Al_{0.5}CoCrCuFeNi$ are very promising.

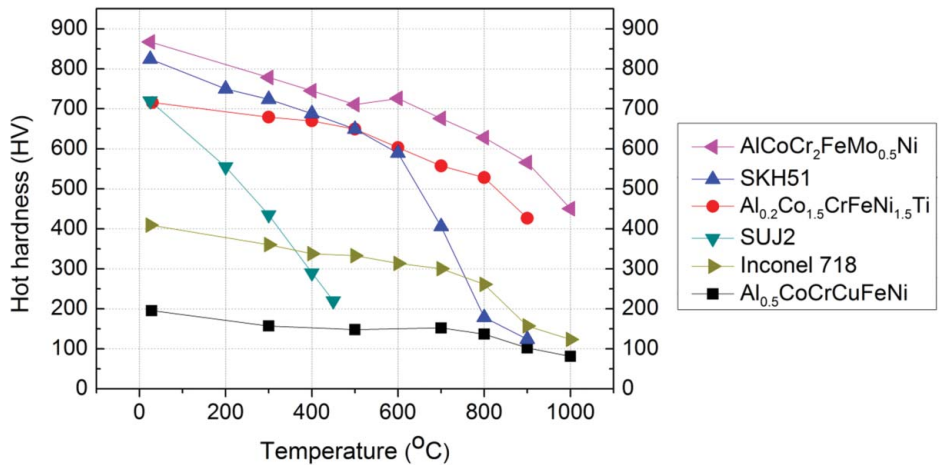

Figure 10. Hardness of various HEAs and conventional alloys as functions of temperature. Some of the data is collected from literature.[50,85]

Downloaded by [Isfahan University of Technology] at 07:20 25 June 2015

5. High Temperatures Properties and Structural Stability Many HEAs have exceptional high-temperature strength/hardness, which originates from their excellent resistance to thermal softening. Figure 10 shows the hot hardness of three HEAs and three conventional alloys as functions of temperature.[50,85] The $AlCoCr_2FeMo_{0.5}Ni$ and $Al_{0.2}Co_{1.5}CrFeNi_{1.5}Ti$ alloys have very high hardness at room temperature (more than two times higher than Inconel 718 superalloy). Their hardness decreases slowly with the increase of temperature. SKH51 and SUJ2 also have very high hardness at room temperature (over HV 700). However, in contrast to the gradual softening behavior for the two HEAs, SKH51 and SUJ2 start to soften drastically at 200 and 600°C, respectively. This leads to a significant difference in hardness for the four alloys at 800°C—the two HEAs are still more than two times harder than the Inconel 718 superalloy, while the two conventional alloys become apparently softer than Inconel 718 (Figure 10). At 1000°C, $AlCoCr_2FeMo_{0.5}Ni$ is already more than three times harder than Inconel 718. Also note that even the soft, sole-FCC $Al_{0.5}CoCrCuFeNi$ alloy is quite resistant to thermal softening.

Hsu et al. [85] calculated the high-temperature softening coefficient of the $AlCoCr_xFeMo_{0.5}Ni$ ($x = 0$–2.0) alloys from the hot hardness vs. temperature curves and found that above the transition temperature (onset temperature for rapid softening), the softening coefficient of these HEAs are evidently lower than that of conventional high-temperature alloys such as Inconel 718 and T800 (Table 3).[85] Softening coefficient of some alloys are even less than half that of Inconel 718. The resistance to thermal softening is mainly a result of the sluggish diffusion in HEAs. Above the transition temperature, deformation proceeds via diffusion-related mechanisms. Thus, the slower diffusion rate in HEAs can effectively reduce the degree of thermal softening.

Table 3. Softening coefficient of two $AlCoCr_xFeMo_{0.5}Ni$ alloys and two conventional high-temperature alloys above transition temperature (T_T).[85]

Alloy	Softening coefficient above T_T
Cr-1.5	−2.32E-4
Cr-2	−1.66E-4
T-800	−3.12E-4
In 718	−3.55E-4

Because the transition temperature and diffusion rate of metallic materials are directly related to the melting point of the material, it can be expected that refractory HEAs should have outstanding properties in this regard. Indeed, W-containing refractory HEAs have excellent resistance to thermal softening. This is shown in Figure 11.[101] The yield strengths

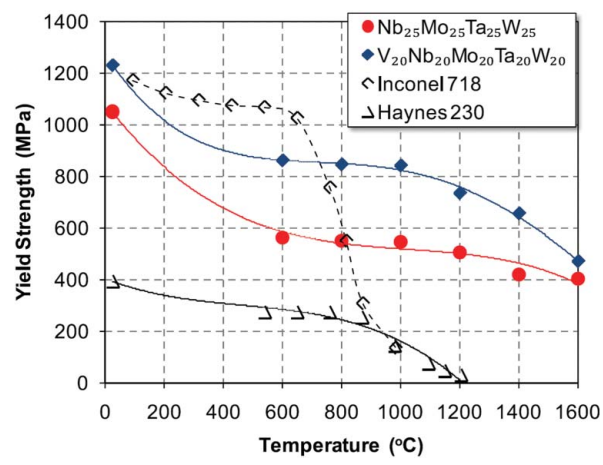

Figure 11. Yield strength as functions of temperature for the $Nb_{25}Mo_{25}Ta_{25}W_{25}$ and $V_{20}Nb_{20}Mo_{20}Ta_{20}W_{20}$ alloys and two superalloys.[101]

Downloaded by [Isfahan University of Technology] at 07:20 25 June 2015

of $Nb_{25}Mo_{25}Ta_{25}W_{25}$ and $V_{20}Nb_{20}Mo_{20}Ta_{20}W_{20}$ alloys remain virtually unchanged in the range of 600–1000°C. The two alloys have extremely high yield strength of over 400 MPa at 1600°C. Owing to their good strength at high temperatures, some refractory alloys actually have higher specific yield strength than superalloys such as Inconel 718 and Haynes 230 at higher than 1000°C.[106]

Structural stability is an important issue for high-temperature applications. HEAs generally have good structural stability at high temperatures. This is owing to (1) slower kinetics due to the sluggish diffusion effect (Section 2.2); (2) reduced driving force to eliminate defects (e.g. grain boundaries, interfaces, etc.). The driving force to eliminate defects originates from the free energy difference between defect-containing and defect-free crystals. However, the defect-free lattice in HEAs is still highly strained and full of atomic-scale zigzag, owing to the atomic size differences between the elements. The strain energy of the distorted lattice raises the overall free energy, leading to a reduced energy difference between defect-containing crystal/amorphous structure and the defect-free crystal.[23,108] Thus, the driving force to eliminate defects is reduced. There is much evidence for the good structural stability of HEAs. For example, the activation energy of grain growth for the CoCrFeMnNi alloy (which has a sole FCC structure) is 321.7 kJ/mole^{-1}.[88] This value is twice that of AISI 304LN, indicating a significantly slower kinetics for microstructural coarsening.[88] Growth of precipitates in HEAs is also slow. Precipitates in HEAs treated at moderate temperature (e.g. 700–800°C) often still remain small—diameters on the scale of tens or hundreds of nanometers have been reported.[34,82] Another example is the NbSiTaTiZr amorphous alloy. The crystallization temperature of NbSiTaTiZr is higher than 800°C.[23] This temperature of stability is probably the highest among reported amorphous metals. The excellent structural stability comes not just from the above two reasons. NbSiTaTiZr was designed based on a free energy consideration.[23] Its composition was selected so that the non-crystalline random solid solution state has a low free energy. This lowers its driving force to crystallize into silicides. Additionally, the kinetics in this alloy is further slowed due to the high atomic packing density and high melting points of composing elements.

6. Corrosion Properties The corrosion resistances of some HEAs have been tested in both NaCl and H_2SO_4 solutions.[20,73,109–121] In both solutions, some HEAs show better corrosion properties than 304 SS and even 304L SS and have good resistance to pitting.[109,115–117] Important factors include alloy composition and microstructure, particularly the amount and distribution of corrosion-resistant elements (such as Cr), and the presence of galvanic corrosion. Most of these tested alloys are based on Co, Cr, Fe and Ni. Therefore, the corrosion behavior of the Co–Cr–Fe–Ni alloys is discussed first, followed by the effect of elemental addition to the alloy system.

Corrosion in NaCl Solution: In NaCl solution, the CoCrFeNi single-phase FCC alloy has markedly better corrosion resistance than 304L SS.[111] This is probably owing to its high Cr and Ni content. Addition of Cu to the CoCrFeNi alloy leads to the formation of Cu-rich interdendrite phase, which suffers from galvanic corrosion and severely degrades the corrosion resistance.[111,118] To make things worse, the passive film on the Cu-rich interdendrite regions does not offer good protection, which further narrows down the passivation region.[111] The corrosion property can be improved by reducing the amount of Cu-rich phase via high-temperature annealing.[118] Addition of 0.5 mole fraction of Al to the CoCrFeNi alloy leads to the formation of (Al, Ni)-rich BCC phase and causes galvanic corrosion in NaCl solution.[73] Al is also detrimental to the corrosion resistance of the $Al_xCrFe_{1.5}MnNi_{0.5}$ alloys. Addition of Al significantly reduces the pitting potential and increases the area of localized/pitting corrosion of these alloys in NaCl solution.[114] Although it has higher pitting potential, the passive region is less than that of 304SS. Addition of Mo to the $Co_{1.5}CrFeNi_{1.5}Ti_{0.5}Mo_x$ alloy is beneficial because it evidently raises the pitting potential.[115,119] For example, $Co_{1.5}CrFeNi_{1.5}Ti_{0.5}Mo_{0.1}$ alloy has a wide passivation region of 1.43 V in 1 M NaCl and does not suffer from any pitting.[116,119]

Corrosion in H_2SO_4 Solution: In H_2SO_4 solution, CoCrFeNi also has better corrosion resistance than 304 SS.[117] Addition of Cu to the CoCrFeNi alloy deteriorates its corrosion properties. Similar to the case in NaCl solution, this is due to the formation of the Cu-rich phase. The width of the passivation region is also evidently narrowed.[109,113] Addition of Al is also harmful.[114,117] It leads to the formation of a FCC+BCC or BCC+B2 two-phase structure, in which the Ni,Al-rich BCC/B2 phase is preferentially corroded.[74,117] Additionally, the existence of Al turns the passive film porous and less protective.[117] Replacing Co with Mn in the Co–Cr–Fe–Ni alloy degrades its corrosion resistance in H_2SO_4 solution, and renders its resistance inferior to 304 SS.[114] Addition of B to the $Al_{0.5}CoCrCuFeNi$ alloy leads to the formation of Cr-rich borides and apparently lowers the Cr content in the matrix.[113] This renders the matrix much less corrosion resistant. Addition of Ti to the Co–Cr–Fe–Ni alloy does not affect its outstanding corrosion behavior.[119] Addition of Mo to the Co–Cr–Fe–Ni–Ti alloy is detrimental to the corrosion resistance in H_2SO_4 solution. This is because of the formation of the (Cr, Mo)-rich σ phase, which reduces the concentration of Cr in other phases.[119] The $AlCu_{0.5}CoCrFeNiSi$ alloy has better general corrosion resistance than 304 SS, but its passivation region is smaller.[109]

Downloaded by [Isfahan University of Technology] at 07:20 25 June 2015

7. Outstanding Issues and Future Directions HEA is an immense field with a countless number of new alloy systems. Our understanding of these new materials is still very limited and preliminary. As mentioned in Section 4, our knowledge mainly focuses on the Al-Co-Cr-Cu-Fe-Ni system, its derivatives, and the refractory HEAs—just a very tiny fraction of the whole HEA world. More elements and combinations need to be explored to further understand the potentials of HEAs. For example, light HEAs are of great interest.[122–124] Non-metallic elements such as C, B, and N can also be incorporated to achieve even higher strength.[14,99,100,125,126] Additionally, HEAs can also be prepared by other process and/or in other forms. For example, HEAs can be processed by a wrought process including homogenization, hot/cold working, and annealing [62,64] to eliminate casting defects and improve microstructure. HEA powders can be prepared by ball milling.[98,127–131] The powders can subsequently be sintered to form bulk HEAs with ultrafine structure.[98,127,129] Single-crystal of the $Al_{0.3}CoCrFeNi$ HEA has also been prepared successfully by the Bridgman solidification method.[132] Cemented carbides and cermets could be sintered by a proper HEA binder to reduce cost and improve resistance to softening. HEA coatings/claddings can also be prepared by sputtering or other cladding techniques.[22,23,73,133–140]

In terms of the phase and crystal structure of HEAs, most of our knowledge is based on the as-cast state (after vacuum arc melting). Very little is known about the equilibrium phases and phase diagrams, but these are key to the design and development of HEAs. Significantly more combined experimental and computational works are needed in this regard. It is worth mentioning that although equimolar compositions are usually the easiest access to a new alloy system, they probably do not possess the best combination of properties. Therefore, there is probably far more treasure in those non-equimolar alloys with carefully designed composition and tailored microstructures. A good approach is to start from equimolar alloys and then extract the desired non-equimolar composition from the equimolar alloy.

The mechanical properties of HEAs available are mostly about hardness and compressive properties. Because reasonable ductility is crucial to structural applications, more studies on tensile behaviors are definitely needed. Additionally, except for a few examples,[57–59,141] not much is known about the deformation of HEAs, e.g. dislocation behavior, deformation twinning, deformation microstructures, texture evolution, stacking fault energy, etc. This information is the foundation for a thorough understanding of mechanical properties. Microstructural characterization in most works is only conducted by SEM. This is not sufficient for unraveling the structure-property relationship in HEAs because all detailed microstructure observations reveal the existence of nano-sized or even atomic-scale precipitations and/or decompositions.[21,31,32,34,35,98,142] More tests aimed at prolonged service and/or high-temperature applications are also required. These include but are not limited to: fatigue behavior,[67] oxidation resistance,[50,51,104] structural stability, and creep behavior.

HEAs can also be used in other applications. For example, HEAs can be used as hydrogen storage materials,[143,144] radiation resistant materials,[145] diffusion barriers for electronics,[22,23] precision resistors,[4,146] electromagnetic shielding materials, soft magnetic materials,[147] thermoelectric materials, functional coatings, and anti-bacterial materials. Because of the distinct design strategy and unique properties, HEAs and other high-entropy materials (e.g. high-entropy ceramics or even polymers) will probably find applications in fields significantly wider than those listed above. This exciting new virgin field awaits exploration by more scientists.

Acknowledgements MH Tsai gratefully thanks the financial support from the National Science Council of Taiwan under grant NSC 102-2218-E-005-004. The authors acknowledge the valuable discussions with Yih-Farn Kao, Sheng-Chieh Liao, and Dr Kun-Yo Tsai.

References

[1] Huang KH, Yeh JW. A study on multicomponent alloy systems containing equal-mole elements [M.S. thesis]. Hsinchu: National Tsing Hua University; 1996.
[2] Yeh JW, Chen SK, Lin SJ, Gan JY, Chin TS, Shun TT, Tsau CH, Chang SY. Nanostructured high-entropy alloys with multiple principal elements: novel alloy design concepts and outcomes. Adv Eng Mater. 2004;6:299–303.
[3] Yeh JW. Recent progress in high-entropy alloys. Ann Chim-Sci Mat. 2006;31:633–648.
[4] Tsai MH. Physical properties of high entropy alloys. Entropy. 2013;15:5338–5345.
[5] Yeh JW. Alloy design strategies on high-entropy alloys. JOM. 2013.
[6] Gaskell DR. Introduction to the thermodynamics of materials. 3rd ed. Washinton (DC): Taylor & Francis; 1995.
[7] Tong CJ, Chen MR, Chen SK, Yeh JW, Shun TT, Lin SJ, Chang SY. Mechanical performance of the $Al_xCoCrCuFeNi$ high-entropy alloy system with multiprincipal elements. Metall Mater Trans A. 2005;36:1263–1271.
[8] Tong CJ, Chen YL, Chen SK, Yeh JW, Shun TT, Tsau CH, Lin SJ, Chang SY. Microstructure characterization of $Al_xCoCrCuFeNi$ high-entropy alloy system with multiprincipal elements. Metall Mater Trans A. 2005;36:881–893.
[9] Li A, Zhang X. Thermodynamic analysis of the simple microstructure of AlCrFeNiCu high-entropy alloy with multi-principal elements. Acta Metallurgica Sinica (English Letters). 2009;22:219–224.
[10] Senkov ON, Wilks GB, Miracle DB, Chuang CP, Liaw PK. Refractory high-entropy alloys. Intermetallics. 2010;18:1758–1765.

Downloaded by [Isfahan University of Technology] at 07:20 25 June 2015

[11] del Grosso MF, Bozzolo G, Mosca HO. Determination of the transition to the high entropy regime for alloys of refractory elements. J Alloys Compd. 2012;534: 25–31.

[12] Ng C, Guo S, Luan J, Shi S, Liu CT. Entropy-driven phase stability and slow diffusion kinetics in an $Al_{0.5}CoCrCuFeNi$ high entropy alloy. Intermetallics. 2012;31:165–172.

[13] Lucas MS, Wilks GB, Mauger L, Munoz JA, Senkov ON, Michel E, Horwath J, Semiatin SL, Stone MB, Abernathy DL, Karapetrova E. Absence of long-range chemical ordering in equimolar FeCoCrNi. Appl Phys Lett. 2012;100:251907.

[14] Hsu CY, Yeh JW, Chen SK, Shun TT. Wear resistance and high-temperature compression strength of Fcc $CuCoNiCrAl_{0.5}Fe$ alloy with boron addition. Metall Mater Trans A. 2004;35:1465–1469.

[15] Zhang KB, Fu ZY. Effects of annealing treatment on phase composition and microstructure of $CoCrFeNiTiAl_x$ high-entropy alloys. Intermetallics. 2012;22:24–32.

[16] Otto F, Yang Y, Bei H, George EP. Relative effects of enthalpy and entropy on the phase stability of equiatomic high-entropy alloys. Acta Mater. 2013;61: 2628–2638.

[17] Lin CW, Tsai MH, Tsai CW, Yeh JW, Chen SK. Microstructure and aging behavior of $Al_5Cr_{32}Fe_{35}Ni_{22}Ti_6$ ternary-like high-entropy alloy. In preparation.

[18] Cheng KH, Lai CH, Lin SJ, Yeh JW. Recent progress in multi-element alloy and nitride coatings sputtered from high-entropy alloy targets. Ann Chim-Sci Mat. 2006;31:723–736.

[19] Tsai KY, Tsai MH, Yeh JW. Sluggish diffusion in Co–Cr–Fe–Mn–Ni high-entropy alloys. Acta Mater. 2013;61:4887–4897.

[20] Chen YY, Duval T, Hong UT, Yeh JW, Shih HC, Wang LH, Oung JC. Corrosion properties of a novel bulk $Cu_{0.5}NiAlCoCrFeSi$ glassy alloy in 288°C high-purity water. Mater Lett. 2007;61:2692–2696.

[21] Singh S, Wanderka N, Murty BS, Glatzel U, Banhart J. Decomposition in multi-component AlCoCrCuFeNi high-entropy alloy. Acta Mater. 2011;59: 182–190.

[22] Tsai MH, Yeh JW, Gan JY. Diffusion barrier properties of AlMoNbSiTaTiVZr high-entropy alloy layer between copper and silicon. Thin Solid Films. 2008;516: 5527–5530.

[23] Tsai MH, Wang CW, Tsai CW, Shen WJ, Yeh JW, Gan JY, Wu WW. Thermal stability and performance of NbSiTaTiZr high-entropy alloy barrier for copper metallization. J Electrochem Soc. 2011;158:H1161–H1165.

[24] Ferro P, Saccone A. Structure of intermetallic compounds and phases. In: Cahn RW, Haasen P, editors. Physical metallurgy. 4th ed. Amsterdam, the Netherlands: Elsevier Science B.V.; 1996.

[25] Cahn RW, Haasen P, editors. Physical Metallurgy. 4th ed. Amsterdam: Elsevier Science B.V.; 1996.

[26] Zhang Y, Zhou YJ, Lin JP, Chen GL, Liaw PK. Solid-solution phase formation rules for multi-component alloys. Adv Eng Mater. 2008;10:534–538.

[27] Guo S, Liu CT. Phase stability in high entropy alloys: formation of solid-solution phase or amorphous phase. Prog Nat Sci: Mater Int. 2011;21:433–446.

[28] Chen ST, Yeh JW. Effect of mixing enthalpy, mixing entropy and atomic size difference on the structure of multicomponent alloys [M.S. thesis]. Hsinchu: National Tsing Hua University; 2009.

[29] Yang X, Zhang Y. Prediction of high-entropy stabilized solid-solution in multi-component alloys. Mater Chem Phys. 2012;132:233–238.

[30] Tsai KY, Tsai MH, Yeh JW. To be submitted.

[31] Manzoni A, Daoud H, Mondal S, van Smaalen S, Völkl R, Glatzel U, Wanderka N. Investigation of phases in $Al_{23}Co_{15}Cr_{23}Cu_8Fe_{15}Ni_{16}$ and $Al_8Co_{17}Cr_{17}Cu_8Fe_{17}Ni_{33}$ high entropy alloys and comparison with equilibrium phases predicted by Thermo-Calc. J Alloys Compd. 2013;552:430–436.

[32] Manzoni A, Daoud H, Völkl R, Glatzel U, Wanderka N. Phase separation in equiatomic AlCoCrFeNi high-entropy alloy. Ultramicroscopy. 2013;132:212–215.

[33] Wang YP, Li BS, Fu HZ. Solid solution or intermetallics in a high-entropy alloy. Adv Eng Mater. 2009;11: 641–644.

[34] Tsai MH, Yuan H, Cheng G, Xu W, Jian WW, Chuang MH, Juan CC, Yeh AC, Lin SJ, Zhu Y. Significant hardening due to the formation of a sigma phase matrix in a high entropy alloy. Intermetallics. 2013;33:81–86.

[35] Tsai MH, Yuan H, Cheng G, Xu W, Tsai KY, Tsai CW, Jian WW, Juan CC, Shen WJ, Chuang MH, Yeh JW, Zhu YT. Morphology, structure and composition of precipitates in $Al_{0.3}CoCrCu_{0.5}FeNi$ high-entropy alloy. Intermetallics. 2013;32:329–336.

[36] Tung CC, Yeh JW, Shun TT, Chen SK, Huang YS, Chen HC. On the elemental effect of AlCoCrCuFeNi high-entropy alloy system. Mater Lett. 2007;61:1–5.

[37] Senkov ON, Scott JM, Senkova SV, Miracle DB, Woodward CF. Microstructure and room temperature properties of a high-entropy TaNbHfZrTi alloy. J Alloys Compd. 2011;509:6043–6048.

[38] Guo S, Ng C, Lu J, Liu CT. Effect of valence electron concentration on stability of fcc or bcc phase in high entropy alloys. J Appl Phys. 2011;109:103505.

[39] Inoue A. Stabilization of metallic supercooled liquid and bulk amorphous alloys. Acta Mater. 2000;48:279–306.

[40] Xia MX, Zhang SG, Ma CL, Li JG. Evaluation of glass-forming ability for metallic glasses based on order-disorder competition. Appl Phys Lett. 2006;89:091917.

[41] Guo S, Hu Q, Ng C, Liu CT. More than entropy in high-entropy alloys: forming solid solutions or amorphous phase. Intermetallics. 2013;41:96–103.

[42] Chen YY, Hong UT, Yeh JW, Shih HC. Mechanical properties of a bulk $Cu_{0.5}NiAlCoCrFeSi$ glassy alloy in 288°C high-purity water. Appl Phys Lett. 2005;87:261918.

[43] Gao XQ, Zhao K, Ke HB, Ding DW, Wang WH, Bai HY. High mixing entropy bulk metallic glasses. J Non-Cryst Solids. 2011;357:3557–3560.

[44] Zhao K, Xia XX, Bai HY, Zhao DQ, Wang WH. Room temperature homogeneous flow in a bulk metallic glass with low glass transition temperature. Appl Phys Lett. 2011;98:141913.

[45] Cunliffe A, Plummer J, Figueroa I, Todd I. Glass formation in a high entropy alloy system by design. Intermetallics. 2012;23:204–207.

[46] Ding HY, Yao KF. High entropy $Ti_{20}Zr_{20}Cu_{20}Ni_{20}Be_{20}$ bulk metallic glass. J Non-Cryst Solids. 2013;364:9–12.

[47] Takeuchi A, Chen N, Wada T, Yokoyama Y, Kato H, Inoue A, Yeh JW. $Pd_{20}Pt_{20}Cu_{20}Ni_{20}P_{20}$ high-entropy alloy as a bulk metallic glass in the centimeter. Intermetallics. 2011;19:1546–1554.

[48] Li HF, Xie XH, Zhao K, Wang YB, Zheng YF, Wang WH, Qin L. In vitro and in vivo studies on biodegradable CaMgZnSrYb high-entropy bulk metallic glass. Acta Biomaterialia. 2013;9:8561–8573.

Downloaded by [Isfahan University of Technology] at 07:20 25 June 2015

[49] Wen LH, Kou HC, Li JS, Chang H, Xue XY, Zhou L. Effect of aging temperature on microstructure and properties of AlCoCrCuFeNi high-entropy alloy. Intermetallics. 2009;17:266–269.

[50] Chuang MH, Tsai MH, Wang WR, Lin SJ, Yeh JW. Microstructure and wear behavior of $Al_xCo_{1.5}CrFeNi_{1.5}Ti_y$ high-entropy alloys. Acta Mater. 2011;59: 6308–6317.

[51] Chen ST, Tang WY, Kuo YF, Chen SY, Tsau CH, Shun TT, Yeh JW. Microstructure and properties of age-hardenable $Al_xCrFe_{1.5}MnNi_{0.5}$ alloys. Mater Sci Eng A. 2010;527:5818–5825.

[52] Tsai MH, Tsai KY, Tsai CW, Lee C, Juan CC, Yeh JW. Criterion for sigma phase formation in Cr- and V-containing high-entropy alloys. Mater Res Lett. 2013;1:207–212.

[53] Zhang C, Zhang F, Chen SL, Cao WS. Computational thermodynamics aided high-entropy alloy design. JOM. 2012;64:839–845.

[54] Senkov ON, Senkova SV, Woodward C, Miracle DB. Low-density, refractory multi-principal element alloys of the Cr–Nb–Ti–V–Zr system: Microstructure and phase analysis. Acta Mater. 2013;61:1545–1557.

[55] Shigenobu O, Yoshitaka U, Masanori K. First-principles approaches to intrinsic strength and deformation of materials: perfect crystals, nano-structures, surfaces and interfaces. Modelling and Simulation in Materials Science and Engineering. 2009;17:013001.

[56] Reed-Hill RE, Abbaschian R. Physical metallurgy principles. 3rd ed. PWS-KENT; 1991.

[57] Otto F, Dlouhý A, Somsen C, Bei H, Eggeler G, George EP. The influences of temperature and microstructure on the tensile properties of a CoCrFeMnNi high-entropy alloy. Acta Mater. 2013;61:5743–5755.

[58] Bhattacharjee PP, Sathiaraj GD, Zaid M, Gatti JR, Lee C, Tsai C-W, Yeh J-W. Microstructure and texture evolution during annealing of equiatomic CoCrFeMnNi high-entropy alloy. J Alloys Compd. 2014;587:544–552.

[59] Zaddach AJ, Niu C, Koch CC, Irving DL. Mechanical properties and stacking fault energies of NiFeCrCoMn high-entropy alloy. JOM. 2013;65:1780–1789.

[60] Tsai CW, Chen YL, Tsai MH, Yeh JW, Shun TT, Chen SK. Deformation and annealing behaviors of high-entropy alloy $Al_{0.5}CoCrCuFeNi$. J Alloys Compd. 2009;486:427–435.

[61] Zhang KB, Fu ZY, Zhang JY, Shi J, Wang WM, Wang H, Wang YC, Zhang QJ. Annealing on the structure and properties evolution of the CoCrFeNiCuAl high-entropy alloy. J Alloys Compd. 2010;502:295–299.

[62] Tsai CW, Tsai MH, Yeh JW, Yang CC. Effect of temperature on mechanical properties of $Al_{0.5}CoCrCuFeNi$ wrought alloy. J Alloys Compd. 2010;490:160–165.

[63] Wang FJ, Zhang Y, Chen GL, Davies HA. Tensile and compressive mechanical behavior of a CoCrCu $FeNiAl_{0.5}$ high entropy alloy. Int J Mod Phys B. 2009;23:1254–1259.

[64] Kuznetsov AV, Shaysultanov DG, Stepanov ND, Salishchev GA, Senkov ON. Tensile properties of an AlCrCuNiFeCo high-entropy alloy in as-cast and wrought conditions. Mater Sci Eng A. 2012;533: 107–118.

[65] Kuznetsov AV, Shaysultanov DG, Stepanov ND, Salishchev GA, Senkov ON. Superplasticity of AlCoC rCuFeNi high entropy alloy. Mater Sci Forum. 2013;735: 146–151.

[66] Wu JM, Lin SJ, Yeh JW, Chen SK, Huang YS. Adhesive wear behavior of $Al_xCoCrCuFeNi$ high-entropy alloys as a function of aluminum content. Wear. 2006;261: 513–519.

[67] Hemphill MA, Yuan T, Wang GY, Yeh JW, Tsai CW, Chuang A, Liaw PK. Fatigue behavior of $Al_{0.5}CoCrCuFeNi$ high entropy alloys. Acta Mater. 2012;60:5723–5734.

[68] Liu ZY, Guo S, Liu XJ, Ye JC, Yang Y, Wang XL, Yang L, An K, Liu CT. Micromechanical characterization of casting-induced inhomogeneity in an $Al_{0.8}CoCrCuFeNi$ high-entropy alloy. Scr Mater. 2011;64:868–871.

[69] Shun TT, Du YC. Microstructure and tensile behaviors of FCC $Al_{0.3}CoCrFeNi$ high entropy alloy. J Alloys Compd. 2009;479:157–160.

[70] Wang WR, Wang WL, Wang SC, Tsai YC, Lai CH, Yeh JW. Effects of Al addition on the microstructure and mechanical property of $Al_xCoCrFeNi$ high-entropy alloys. Intermetallics. 2012;26:44–51.

[71] Kao YF, Chen TJ, Chen SK, Yeh JW. Microstructure and mechanical property of as-cast, -homogenized, and -deformed $Al_xCoCrFeNi$ ($0 \leq x \leq 2$) high-entropy alloys. J Alloys Compd. 2009;488:57–64.

[72] Li C, Li JC, Zhao M, Jiang Q. Effect of aluminum contents on microstructure and properties of $Al_xCoCrFeNi$ alloys. J Alloys Compd. 2010;504:S515–S518.

[73] Lin CM, Tsai HL. Evolution of microstructure, hardness, and corrosion properties of high-entropy $Al_{0.5}CoCrFeNi$ alloy. Intermetallics. 2011;19:288–294.

[74] Wang YP, Li BS, Ren MX, Yang C, Fu HZ. Microstructure and compressive properties of AlCrFe-CoNi high entropy alloy. Mater Sci Eng A. 2008;491: 154–158.

[75] Chen MR, Lin SJ, Yeh JW, Chen SK, Huang YS, Tu CP. Microstructure and properties of $Al_{0.5}CoCrCuFeNiTi_x$ ($x = 0$–2.0) high-entropy alloys. Mater Trans. 2006;47: 1395–1401.

[76] Shun TT, Chang LY, Shiu MH. Microstructures and mechanical properties of multiprincipal component $CoCrFeNiTi_x$ alloys. Mater Sci Eng A. 2012;556: 170–174.

[77] Zhou YJ, Zhang Y, Wang YL, Chen GL. Solid solution alloys of $AlCoCrFeNiTi_x$ with excellent room-temperature mechanical properties. Appl Phys Lett. 2007;90:181904.

[78] Wang XF, Zhang Y, Qiao Y, Chen GL. Novel microstructure and properties of multicomponent $CoCrCuFeNiTi_x$ alloys. Intermetallics. 2007;15:357–362.

[79] Zhang KB, Fu ZY, Zhang JY, Wang WM, Wang H, Wang YC, Zhang QJ, Shi J. Microstructure and mechanical properties of $CoCrFeNiTiAl_x$ high-entropy alloys. Mater Sci Eng A. 2009;508:214–219.

[80] Hsu CY, Sheu TS, Yeh JW, Chen SK. Effect of iron content on wear behavior of $AlCoCrFe_xMo_{0.5}Ni$ high-entropy alloys. Wear. 2010;268:653–659.

[81] Hsu CY, Wang WR, Tang WY, Chen SK, Yeh JW. Microstructure and mechanical properties of new $AlCo_xCrFeMo_{0.5}Ni$ high-entropy alloys. Adv Eng Mater. 2010;12:44–49.

[82] Shun TT, Hung CH, Lee CF. The effects of secondary elemental Mo or Ti addition in $Al_{0.3}CoCrFeNi$ high-entropy alloy on age hardening at 700°C. J Alloys Compd. 2010;495:55–58.

[83] Zhu JM, Zhang HF, Fu HM, Wang AM, Li H, Hu ZQ. Microstructures and compressive properties of multicomponent $AlCoCrCuFeNiMo_x$ under-bar alloys. J Alloys Compd. 2010;497:52–56.

[84] Zhu JM, Fu HM, Zhang HF, Wang AM, Li H, Hu ZQ. Microstructures and compressive properties of

multicomponent $AlCoCrFeNiMo_x$ alloys. Mater Sci Eng A. 2010;527:6975–6979.
[85] Hsu CY, Juan CC, Wang WR, Sheu TS, Yeh JW, Chen SK. On the superior hot hardness and softening resistance of $AlCoCr_xFeMo_{0.5}Ni$ high-entropy alloys. Mater Sci Eng A. 2011;528:3581–3588.
[86] Shun TT, Chang LY, Shiu MH. Microstructure and mechanical properties of multiprincipal component $CoCrFeNiMo_x$ alloys. Mater Charact. 2012;70:63–67.
[87] Juan CC, Hsu CY, Tsai CW, Wang WR, Sheu TS, Yeh JW, Chen SK. On microstructure and mechanical performance of $AlCoCrFeMo_{0.5}Ni_x$ high-entropy alloys. Intermetallics. 2013;32:401–407.
[88] Liu WH, Wu Y, He JY, Nieh TG, Lu ZP. Grain growth and the Hall-Petch relationship in a high-entropy FeCrNiCoMn alloy. Scr Mater. 2013;68:526–529.
[89] Tsao LC, Chen CS, Chu CP. Age hardening reaction of the $Al_{0.3}CrFe_{1.5}MnNi_{0.5}$ high entropy alloy. Mater Des. 2012;36:854–858.
[90] Zhu JM, Fu HM, Zhang HF, Wang AM, Li H, Hu ZQ. Synthesis and properties of multiprincipal component $AlCoCrFeNiSi_x$ alloys. Mater Sci Eng A. 2010;527:7210–7214.
[91] Zhuang YX, Liu WJ, Chen ZY, Xue HD, He JC. Effect of elemental interaction on microstructure and mechanical properties of FeCoNiCuAl alloys. Mater Sci Eng A. 2012;556:395–399.
[92] Ma SG, Zhang Y. Effect of Nb addition on the microstructure and properties of AlCoCrFeNi high-entropy alloy. Mater Sci Eng A. 2012;532:480–486.
[93] Li BS, Wang YR, Ren MX, Yang C, Fu HZ. Effects of Mn, Ti and V on the microstructure and properties of AlCrFeCoNiCu high entropy alloy. Mater Sci Eng A. 2008;498:482–486.
[94] Chen MR, Lin SJ, Yeh JW, Chen SK, Huang YS, Chuang MH. Effect of vanadium addition on the microstructure, hardness, and wear resistance of $Al_{0.5}CoCrCuFeNi$ high-entropy alloy. Metall Mater Trans A. 2006;37: 1363–1369.
[95] Hu ZH, Zhan YZ, Zhang GH, She J, Li CH. Effect of rare earth Y addition on the microstructure and mechanical properties of high entropy AlCoCrCuNiTi alloys. Mater Des. 2010;31:1599–1602.
[96] Liu L, Zhu JB, Li L, Li JC, Jiang Q. Microstructure and tensile properties of $FeMnNiCuCoSn_x$ high entropy alloys. Mater Des. 2013;44:223–227.
[97] Liu L, Zhu JB, Zhang C, Li JC, Jiang Q. Microstructure and the properties of $FeCoCuNiSn_x$ high entropy alloys. Mater Sci Eng A. 2012;548:64–68.
[98] Pradeep KG, Wanderka N, Choi P, Banhart J, Murty BS, Raabe D. Atomic-scale compositional characterization of a nanocrystalline AlCrCuFeNiZn high-entropy alloy using atom probe tomography. Acta Mater. 2013;61:4696–4706.
[99] Shun TT, Du YC. Age hardening of the $Al_{0.3}CoCrFeNiC_{0.1}$ high entropy alloy. J Alloys Compd. 2009;478: 269–272.
[100] Zhu JM, Fu HM, Zhang HF, Wang AM, Li H, Hu ZQ. Microstructure and compressive properties of multiprincipal component $AlCoCrFeNiC_x$ alloys. J Alloys Compd. 2011;509:3476–3480.
[101] Senkov ON, Wilks GB, Scott JM, Miracle DB. Mechanical properties of $Nb_{25}Mo_{25}Ta_{25}W_{25}$ and $V_{20}Nb_{20}Mo_{20}Ta_{20}W_{20}$ refractory high entropy alloys. Intermetallics. 2011;19:698–706.
[102] Senkov ON, Woodward CF. Microstructure and properties of a refractory $NbCrMo_{0.5}Ta_{0.5}TiZr$ alloy. Mater Sci Eng A. 2011;529:311–320.
[103] Senkov ON, Scott JM, Senkova SV, Meisenkothen F, Miracle DB, Woodward CF. Microstructure and elevated temperature properties of a refractory TaNbHfZrTi alloy. J Mater Sci. 2012;47:4062–4074.
[104] Senkov ON, Senkova SV, Dimiduk DM, Woodward C, Miracle DB. Oxidation behavior of a refractory $NbCrMo_{0.5}Ta_{0.5}TiZr$ alloy. J Mater Sci. 2012;47: 6522–6534.
[105] Yang X, Zhang Y, Liaw PK. Microstructure and compressive properties of $NbTiVTaAl_x$ high entropy alloys. Procedia Eng. 2012;36:292–298.
[106] Senkov ON, Senkova SV, Miracle DB, Woodward C. Mechanical properties of low-density, refractory multiprincipal element alloys of the Cr–Nb–Ti–V–Zr system. Mater Sci Eng A. 2013;565:51–62.
[107] Chuang MH, Tsai MH, Tsai CW, Yang NH, Chang SY, Yeh JW, Chen SK, Lin SJ. Intrinsic surface hardening and precipitation kinetics of $Al_{0.3}CrFe_{1.5}MnNi_{0.5}$ multi-component alloy. J Alloys Compd. 2013;551: 12–18.
[108] Huang PK, Yeh JW. Inhibition of grain coarsening up to 1000°C in (AlCrNbSiTiV)N superhard coatings. Scr Mater. 2010;62:105–108.
[109] Chen YY, Duval T, Hung UD, Yeh JW, Shih HC. Microstructure and electrochemical properties of high entropy alloys—a comparison with type-304 stainless steel. Corros Sci. 2005;47:2257–2279.
[110] Chen YY, Hong UT, Shih HC, Yeh JW, Duval T. Electrochemical kinetics of the high entropy alloys in aqueous environments—a comparison with type 304 stainless steel. Corros Sci. 2005;47:2679–2699.
[111] Hsu YJ, Chiang WC, Wu JK. Corrosion behavior of $FeCoNiCrCu_x$ high-entropy alloys in 3.5% sodium chloride solution. Mater Chem Phys. 2005;92:112–117.
[112] Chen YY, Hong UT, Yeh JW, Shih HC. Selected corrosion behaviors of a $Cu_{0.5}NiAlCoCrFeSi$ bulk glassy alloy in 288°C high-purity water. Scr Mater. 2006;54: 1997–2001.
[113] Lee CP, Chen YY, Hsu CY, Yeh JW, Shih HC. The effect of boron on the corrosion resistance of the high entropy alloys $Al_{0.5}CoCrCuFeNiB_x$. J Electrochem Soc. 2007;154:C424–C430.
[114] Lee CP, Chang CC, Chen YY, Yeh JW, Shih HC. Effect of the aluminium content of $Al_xCrFe_{1.5}MnNi_{0.5}$ high-entropy alloys on. the corrosion behaviour in aqueous environments. Corros Sci. 2008;50:2053–2060.
[115] Chou YL, Wang YC, Yeh JW, Shih HC. Pitting corrosion of the high-entropy alloy $Co_{1.5}CrFeNi_{1.5}Ti_{0.5}Mo_{0.1}$ in chloride-containing sulphate solutions. Corros Sci. 2010;52:3481–3491.
[116] Chou YL, Yeh JW, Shih HC. The effect of molybdenum on the corrosion behaviour of the high-entropy alloys $Co_{1.5}CrFeNi_{1.5}Ti_{0.5}Mo_x$ in aqueous environments. Corros Sci. 2010;52:2571–2581.
[117] Kao YF, Lee TD, Chen SK, Chang YS. Electrochemical passive properties of $Al_xCoCrFeNi$ ($x = 0$, 0.25, 0.50, 1.00) alloys in sulfuric acids. Corros Sci. 2010;52: 1026–1034.
[118] Lin CM, Tsai HL, Bor HY. Effect of aging treatment on microstructure and properties of high-entropy $Cu_{0.5}CoCrFeNi$ alloy. Intermetallics. 2010;18: 1244–1250.

Downloaded by [Isfahan University of Technology] at 07:20 25 June 2015

[119] Chou YL, Yeh JW, Shih HC. Effect of molybdenum on the pitting resistance of $Co_{1.5}CrFeNi_{1.5}Ti_{0.5}Mo_x$ alloys in chloride solutions. Corrosion. 2011;67:085002.
[120] Lin CM, Tsai HL. Effect of annealing treatment on microstructure and properties of high-entropy $FeCoNiCrCu_{0.5}$ alloy. Mater Chem Phys. 2011;128: 50–56.
[121] Yu Y, Xie FQ, Zhang TB, Kou HC, Hu R, Li JS. Microstructure control and corrosion properties of $AlCoCrFeNiTi_{0.5}$ high-entropy alloy. Rare Metal Mater Eng. 2012;41:862–866.
[122] Juan CC, Yeh JW, Chin TS, editors. A novel light high-entropy alloy $Al_{20}Be_{20}Fe_{10}Si_{15}Ti_{35}$. E-MRS Fall Meeting 2009; Warsaw, Poland.
[123] Cotton J, Munitz A, Oliver R, Gomes R, Bourne G, Kaufman M, editors. Search for lower density high entropy alloys. TMS2013; 2013; San Antonio, TX.
[124] Kecskes L, Atwater M, Hammond V, Maupin H, Darling K, editors. Influence of processing parameters on the microstructure and mechanical properties of lightweight high entropy alloys. TMS2013; 2013; San Antonio, TX.
[125] Tang WY, Yeh JW. Effect of aluminum content on plasma-nitrided $Al_xCoCrCuFeNi$ high-entropy alloys. Metall Mater Trans A. 2009;40:1479–1486.
[126] Tang WY, Chuang MH, Lin SJ, Yeh JW. Microstructures and mechanical performance of plasma-nitrided $Al_{0.3}CrFe_{1.5}MnNi_{0.5}$ high-entropy alloys. Metall Mater Trans A. 2012;43:2390–2400.
[127] Varalakshmi S, Kamaraj M, Murty BS. Synthesis and characterization of nanocrystalline AlFeTiCrZnCu high entropy solid solution by mechanical alloying. J Alloys Compd. 2008;460:253–257.
[128] Chen Y-L, Hu Y-H, Tsai C-W, Hsieh C-A, Kao S-W, Yeh J-W, Chin T-S, Chen S-K. Alloying behavior of binary to octonary alloys based on Cu–Ni–Al–Co–Cr–Fe–Ti–Mo during mechanical alloying. J Alloys Compd. 2009;477:696–705.
[129] Varalakshmi S, Rao GA, Kamaraj M, Murty BS. Hot consolidation and mechanical properties of nanocrystalline equiatomic AlFeTiCrZnCu high entropy alloy after mechanical alloying. J Mater Sci. 2010;45: 5158–5163.
[130] Varalakshmi S, Kamaraj M, Murty BS. Formation and stability of equiatomic and nonequiatomic nanocrystalline CuNiCoZnAlTi high-entropy alloys by mechanical alloying. Metall Mater Trans A. 2010;41:2703–2709.
[131] Chen Y-L, Tsai C-W, Juan C-C, Chuang M-H, Yeh J-W, Chin T-S, Chen S-K. Amorphization of equimolar alloys with HCP elements during mechanical alloying. J Alloys Compd. 2010;506:210–215.
[132] Ma SG, Zhang SF, Gao MC, Liaw PK, Zhang Y. A successful synthesis of the CoCrFeNiAl0.3 single-crystal, high-entropy alloy by bridgman solidification. JOM. 2013;65:1751–1758.
[133] Chen JH, Hua PH, Chen PN, Chang CM, Chen MC, Wu W. Characteristics of multi-element alloy cladding produced by TIG process. Mater Lett. 2008;62:2490–2492.
[134] Dolique V, Thomann A-L, Brault P, Tessier Y, Gillon P. Complex structure/composition relationship in thin films of AlCoCrCuFeNi high entropy alloy. Mater Chem Phys. 2009;117:142–147.
[135] Dolique V, Thomann AL, Brault P, Tessier Y, Gillon P. Thermal stability of AlCoCrCuFeNi high entropy alloy thin films studied by in-situ XRD analysis. Surf Coat Technol. 2010;204:1989–1992.
[136] Lin YC, Cho YH. Elucidating the microstructure and wear behavior for multicomponent alloy clad layers by in situ synthesis. Surf Coat Technol. 2008;202:4666–4672.
[137] Chen JH, Chen PN, Hua PH, Chen MC, Chang YY, Wu W. Deposition of multicomponent alloys on low-carbon steel using gas tungsten arc welding (GTAW) cladding process. Mater Trans. 2009;50:689–694.
[138] Chen JH, Chen PN, Lin CM, Chang CM, Chang YY, Wu W. Characterization of multi-element alloy claddings manufactured by the tungsten inert gas process. Surf Coat Technol. 2009;203:2983–2988.
[139] Lin YC, Cho YH. Elucidating the microstructural and tribological characteristics of NiCrAlCoCu and NiCrAlCoMo multicomponent alloy clad layers synthesized in situ. Surf Coat Technol. 2009;203:1694–1701.
[140] Zhang H, Pan Y, He YZ. Effects of annealing on the microstructure and properties of 6FeNiCoCrAlTiSi high-entropy alloy coating prepared by laser cladding. J Therm Spray Technol. 2011;20:1049–1055.
[141] Zhu C, Lu ZP, Nieh TG. Incipient plasticity and dislocation nucleation of FeCoCrNiMn high-entropy alloy. Acta Mater. 2013;61:2993–3001.
[142] Singh S, Wanderka N, Kiefer K, Siemensmeyer K, Banhart J. Effect of decomposition of the Cr–Fe–Co rich phase of AlCoCrCuFeNi high entropy alloy on magnetic properties. Ultramicroscopy. 2011;111:619–622.
[143] Kao YF, Chen SK, Sheu JH, Lin JT, Lin WE, Yeh JW, Lin SJ, Liou TH, Wang CW. Hydrogen storage properties of multi-principal-component $CoFeMnTi_xV_yZrz$ alloys. Intl J Hydrog Energy. 2010;35:9046–9059.
[144] Kunce I, Polanski M, Bystrzycki J. Structure and hydrogen storage properties of a high entropy ZrTiVCrFeNi alloy synthesized using Laser Engineered Net Shaping (LENS). Int J Hydrog Energy. 2013;38:12180–12189.
[145] Nagase T, Anada S, Rack PD, Noh JH, Yasuda H, Mori H, Egami T. Electron-irradiation-induced structural change in Zr–Hf–Nb alloy. Intermetallics. 2012;26:122–130.
[146] Chen SK, Kao YF. Near-constant resistivity in 4.2-360 K in a B2 $Al_{2.08}CoCrFeNi$. AIP Adv. 2012;2:012111.
[147] Zhang Y, Zuo T, Cheng Y, Liaw PK. High-entropy alloys with high saturation magnetization, electrical resistivity, and malleability. Sci Rep. 2013;3:1455.

Downloaded by [Isfahan University of Technology] at 07:20 25 June 2015